Phase stabilization by rapid thermal annealing in amorphous hydrogenated silicon nitride film

Sarab Preet Singh[1]**, P Srivastava**[1]**, S Ghosh**[1]**, Saif Ali Khan**[2] **and G Vijaya Prakash**[1,3]

[1] Department of Physics, IIT Delhi, Hauz Khas, New Delhi 110016, India
[2] Inter-University Accelerator Centre, Aruna Asif Ali Marg, New Delhi 110067, India

E-mail: prakash@physics.iitd.ac.in

Abstract
We have studied the effect of rapid thermal annealing (RTA) in the context of phase evolution and stabilization in hydrogenated amorphous silicon nitride (a-SiN$_x$:H) thin films having different stoichiometries, deposited by an Hg-sensitized photo-CVD (chemical vapor deposition) technique. RTA-treated films showed substantial densification and increase in refractive index. Our studies indicate that a mere increase in flow of silicon (Si)-containing gas would not result in silicon-rich a-SiN$_x$:H films. We found that out-diffusion of hydrogen, upon RTA treatment, plays a vital role in the overall structural evolution of the host matrix. It is speculated that less incorporation of hydrogen in as-deposited films with moderate Si content helps in the stabilization of the silicon nitride (Si$_3$N$_4$) phase and may also enable unreacted Si atoms to cluster after RTA. These studies are of great interest in silicon photonics where the post-treatment of silicon-rich devices is essential.

(Some figures in this article are in colour only in the electronic version)

1. Introduction

Silicon-rich dielectrics have attracted much interest in recent years owing to potential applications in optoelectronics technology due to their good stability and compatibility with current microelectronics technology [1]. Subsequent to the observation of intense light emission from porous silicon, silicon nanocrystals (Si-nc) in SiO$_x$ systems have been extensively studied [2, 3]. However, since the injection of charge carriers is limited by the extremely high potential barrier ($\sim$8.5 eV) of silicon dioxide (SiO$_2$), the efficient usage of such a composite is difficult for applications such as electrophotonic devices [4]. In such cases, hydrogenated amorphous silicon nitride (a-SiN$_x$:H), because of its low potential barrier ($\sim$2.0 eV) for carriers, can alleviate the carrier injection problem and hence is considered as a potential candidate for the development of silicon-based photonic devices [5].

Silicon-rich SiO$_x$/SiN$_x$ can be obtained by many fabrication methods such as co-sputtering, plasma-enhanced chemical vapor deposition (PECVD) and high-dose ion implantation [6–10]. The post-annealing process is very crucial for silicon optoelectronics device fabrication and is mainly carried out to obtain phase stabilization/separation in deposited films. In current silicon-based technologies, rapid thermal processing (RTP) is considered to be an efficient alternative process to avoid a range of processing steps and, most importantly, as a cost- and time-effective technology [11].

In general, the structural and optical properties of a-SiN$_x$:H films are strongly affected by the presence of Si–Si, Si–N, Si–H, N–H and Si–O bonds. Therefore, one can further tune the electrical and optical properties by appropriately choosing the parameters for thermal treatment [12–15]. In our recent communication, we reported that optical constants and compaction of the film were found to increase after RTA treatment [16]. It was proposed that hydrogen-terminated defects/voids created due to predominant out-diffusion of hydrogen on RTA treatment are responsible for the aforementioned observations. Such information is

---

[3] Author to whom any correspondence should be addressed.

eventually very important in many optoelectronic device applications, such as optically and/or electrically active Si-based waveguides [1–4]. Hence, a complete and more elaborate study is essential to optimize the entire RTA process. In particular, the increase of crystalline silicon (c-Si) content in the high bandgap material SiN_x is quite promising and would further pave the way for intense opto-electrical studies. To the best of our knowledge, the role of the presence of hydrogen/oxygen in phase-induced segregation of silicon in a-SiN_x:H is, until now, not unambiguously understood.

In the present work, we report a detailed study of structural and optical changes on rapid thermal annealing (RTA) of hydrogenated amorphous silicon nitride (a-SiN_x:H) films prepared by Hg-sensitized photochemical vapor deposition (photo-CVD). The properties of as-deposited and annealed films have been studied by ellipsometry, elastic recoil detection analysis (ERDA), x-ray photoelectron spectroscopy (XPS) and glancing angle x-ray diffraction (GAXRD). Here we have elaborately discussed the structural features of films of different stoichiometries and the possible role of the presence of different phases present such as c-Si, silicon nitride, silicon dioxide and silicon oxynitride (SiO_xN_y) in the as-deposited and annealed films.

2. Experimental details

The hydrogenated amorphous silicon nitride films (a-SiN_x:H) were deposited on an n-type (100) silicon wafer in a Hg-sensitized photo-CVD system (SMCO UVD-10, Japan). In this set-up, reactant gasses pass through a mercury reservoir located outside the reaction chamber with provision of heating up to 200 °C. In the Hg-sensitized process the mercury vapor introduced into the reaction chamber resonantly absorbs UV radiation at 254 nm emitted from a low-pressure mercury lamp and transfers energy to the reactant gases. The basic photo-CVD reaction sequence details were described elsewhere [17]. The reactant gas flow rate ratio $R = SiH_4$ (2% in argon)/NH_3 was modified by varying the partial pressure of silane to deposit films with different stoichiometric compositions, while all the other deposition parameters were kept constant. For post-annealing treatment, we have used rapid thermal annealing (RTA) in nitrogen ambient at 950 °C for 10 s.

As-deposited (hereafter ASD) and rapid thermally annealed (hereafter RTA) film thickness and refractive index were measured by single-wavelength (wavelength 632.8 nm) null-method ellipsometry at an incident angle of 70°.

Glancing angle x-ray diffraction (GAXRD) measurements were carried out using Cu Kα ($\lambda = 1.5418$ Å). Conventional θ–2θ scans between 20° and 80° were typically done at 0.05° steps with a glancing incidence angle of 1°.

Areal concentration of hydrogen (N_H in atoms cm^{-2}) of both ASD-and RTA-treated films was measured by the elastic recoil detection analysis (ERDA) method using Ag^{7+} (100 MeV) ions. ERDA experiments were carried out at a pressure of 4.5×10^{-6} mbar and a collimated beam of silver ions of a spot size of 1×1 mm^2 was made to impact at an angle of 20° with respect to the sample. The hydrogen recoils from the films were detected in a silicon surface barrier

detector (SSBD) kept at 30° recoil angle with a polypropylene stopper foil in front of it to stop other recoils like nitrogen (N), oxygen (O) and silicon (Si). The simulation code transport of ions in matter (TRIM) was used to choose the thickness of the stopper foil. The areal concentration of hydrogen (H) (N_H atoms cm$^{-2} \pm 5\%$) was calculated from the integral counts (Y) of the recoil energy spectra, with the help of the following equation:

$$N = Y \sin \alpha \left(N_p \left(\frac{d\sigma}{d\Omega} \right) \Omega \right)^{-1} \tag{1}$$

where α is the target tilt angle, Ω is the solid angle subtended by the detector and $d\sigma/d\Omega$ is the Rutherford recoil cross section. The data was taken in event-by-event mode with the help of analog-to-digital converters and a fluence-dependent N_H was estimated on-line [18].

The surface phase compositions of the films were analyzed by means of x-ray photoelectron spectroscopy (XPS). The base pressure in the main chamber was 2×10^{-9} mbar and the photoelectrons were excited using an Mg Kα source of energy 1253.6 eV. The accuracy in binding energy determination was 0.05 eV. The carbon 1s (284.6 eV) peak as a reference is used to take care of any shift due to a charging effect. To remove any oxygen and carbon surface contamination, sputtering was carried out for 1 min duration with an Ar$^+$ (5 keV) beam prior to the measurements.

3. Results and discussion

Various hydrogenated amorphous silicon nitride films (a-SiN_x:H) were deposited using different flow rate ratios of reactant gases ($R = SiH_4$ (2% in argon)/NH_3), between $R = 0.02$ and 0.06. Both ASD and RTA films were used for all further investigations.

The refractive index and thickness of ASD and RTA films were measured using the ellipsometry technique and the values are shown in table 1. The thicknesses of ASD films are typically between 350 and 650 Å (± 10 Å) and refractive index values are between 1.75 and 1.90 (± 0.05). It was expected that, with an increase of gas flow rate ratio (R), ASD films should become silicon-rich and therefore would show a high refractive index, but the observed values are lower than that of stoichiometric silicon nitride (Si_3N_4). Since the films were deposited at relatively low temperature (substrate temperature $\sim$200 °C), the incorporation of hydrogen is most likely, which may reduce the refractive index of the ASD films [19]. However, upon RTA treatment, all films showed substantial increase in the refractive index (5–22%) along with the compaction (11–29%) of films (see table 1). For comparison, the film corresponding to $R = 0.04$ showed more densification, whereas films of $R = 0.03$ show high refractive index (2.25). These preliminary studies suggest that a mere change in gas flow rate ratio would not simply result in silicon-rich a-SiN_x:H films. But other factors, such as hydrogen content and phase separation into possible components (namely silicon nitride (Si_3N_4), silicon dioxide (SiO_2) and silicon oxynitride (SiO_xN_y)), may play a vital role. We have performed glancing angle x-ray diffraction (GAXRD)
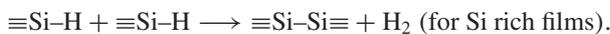
Table 1. Experimental values of gas flow rate ratio ($R = $ SiH$_4$ (2% in argon)/NH$_3$), thickness ($t \pm 10$ Å) and refractive index ($n \pm 0.05$) and their enhancements, Δt and Δn (in %), respectively, and ERDA estimates of hydrogen concentrations ($\pm 0.1 \times 10^{22}$ cm^{-3}) for ASD and RTA (under N$_2$ atmosphere at 950 °C) films.

	As-deposited ASD		Rapid thermal annealed RTA				Hydrogen concentration ($\times 10^{22}$ cm^{-3})	
R	t (Å)	n	t (Å)	n	Δt (%)	Δn (%)	ASD	RTA
0.02	650	1.80	470	2.20	27	22	6.5	0.4
0.03	540	1.90	480	2.25	11	18	8.1	0.5
0.04	480	1.90	340	2.00	29	05	5.8	0.5
0.05	380	1.75	320	2.00	15	17	6.5	0.6
0.06	420	1.75	340	2.15	19	22	7.6	0.5

on both ASD and RTA films (not shown here) to verify the nature of the films. Except for $R = 0.04$ all ASD and RTA films showed no traces of crystallinity and are found to be amorphous in nature. However, for the $R = 0.04$ film, while ASD is amorphous, the corresponding RTA film showed slight traces of the presence of c-Si. In brief, our initial investigations suggest that there is a need to pay attention to other factors like hydrogen content and phase-separated constituents and their role in the a-SiN$_x$:H films, before and after thermal treatment.

Typical variation of hydrogen concentration (atoms cm^{-2}) against incident ion fluence (ions cm^{-2}) of Ag^{7+} (100 MeV) for ASD films of $R = 0.02$ and 0.06 is shown in figures 1(a) and (b), respectively. It has been observed that H content of the film decreases with incident ion fluence. The data is fitted using equation $N_H = N_0 \exp(-\sigma \varphi)$, where N_0 is the initial concentration of hydrogen (atoms cm^{-2}), σ is the hydrogen release cross section (cm^2) and φ is the ion fluence (ions cm^{-2}) [20]. The two slopes indicate that, after a certain fluence, there is a change in the value of the cross section due to overlap of ion-damaged zones. This type of variation has already been studied in polymer materials and a similar model was proposed [20]. However, the initial value of N_H was calculated by extrapolating this graph to the Y axis. Finally, the H concentration (atoms cm^{-3}) of the films was determined by dividing the areal concentration by the thickness of the films (see table 1).

As seen from table 1, in ASD films the amount of hydrogen incorporated for all R values is widely different and independent of stoichiometry. For a comparison, the hydrogen concentration is found to be lowest for the ASD sample with $R = 0.04$, whereas it substantially decreases for all RTA films. It is a clear indicative that out-diffusion of hydrogen takes place during RTA treatment. Hence, one can conclude that out-diffusion of hydrogen due to annealing plays a prominent role in the densification of films. It also further implies that the Si–H and N–H bonds present in ASD films undergo a structural rearrangement upon thermal treatment. The coexistence of these possible structural rearrangements are represented as follows:

$$\equiv\text{Si–H} + =\text{N–H} \longrightarrow \equiv\text{Si–N}= + \text{H}_2 \text{ (for N rich films)}$$

$$\equiv\text{Si–H} + \equiv\text{Si–H} \longrightarrow \equiv\text{Si–Si}\equiv + \text{H}_2 \text{ (for Si rich films)}.$$

Our present investigations are consistent with previous reports of a-SiN$_x$:H films processed using other annealing techniques,
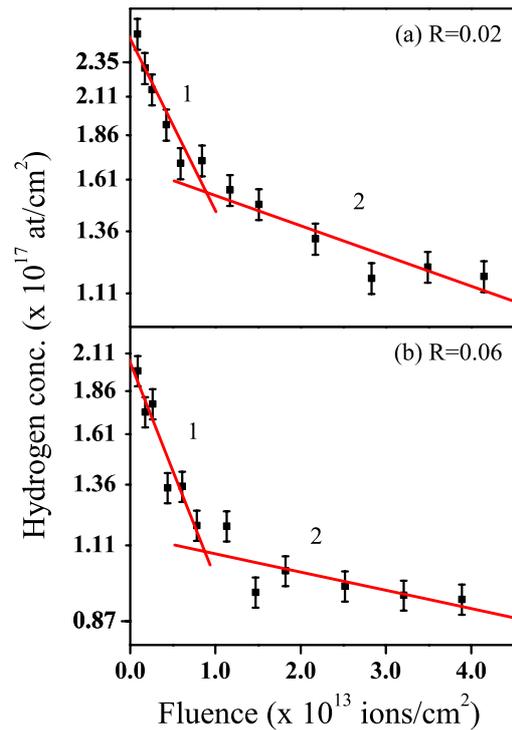

Figure 1. Typical variation of hydrogen concentration with fluence of Ag^{7+} (100 MeV) beam bombarded on ASD hydrogenated amorphous silicon nitride films. Solid lines (red) are linear fits of regions 1 and 2 (see text). Error bars show statistical error in the calculated values.

namely furnace annealing, soft x-ray/VUV and synchrotron radiation irradiation, wherein the densification of films with enhanced refractive index is reported [12, 21–23].

To examine the phase-separated individual silicon entities and to get further insight about the surface composition of the films, x-ray photoelectron spectroscopy (XPS) was used. Here we have examined the core level bonding, particularly the Si 2p and N 1s regions, for all the ASD and RTA films (see figures 2 and 3). Figure 2 represents the XPS data for the Si 2p region for all films under investigation. The Si 2p peak for all the films, in general, has a large peak width, indicating the presence of more than one component. Hence each peak was deconvoluted using a Gaussian curve fitting method into chemically shifted components. These peak shifts are due to charge transfer from the Si to their electronegative ligand (either N or O atoms).
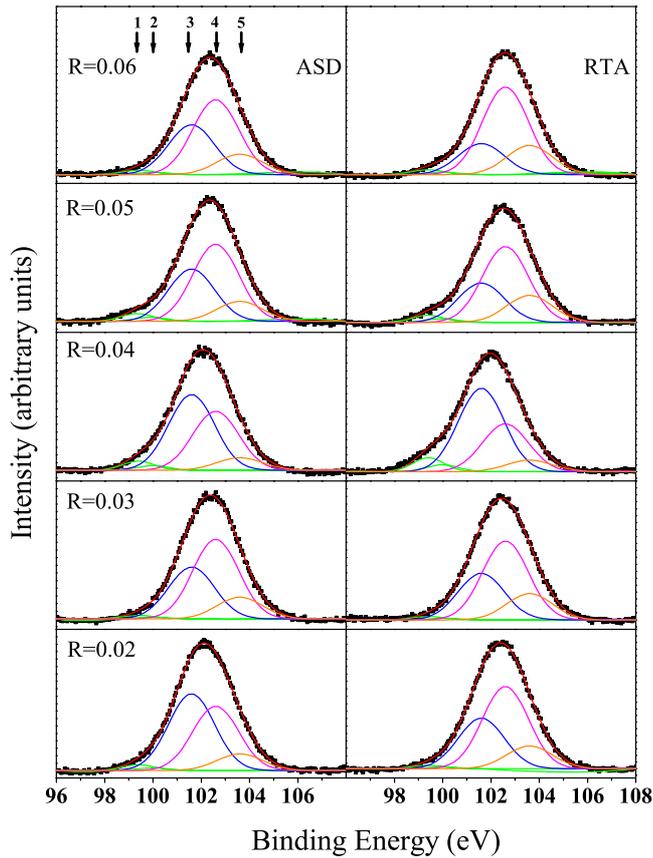
Figure 2. Si 2p XPS spectra of ASD and RTA films for different values of gas flow rate ratio R. The experimental data has been deconvoluted into peaks 1 and 2 corresponding to elemental Si, whereas peaks 3, 4 and 5 represent Si in Si_3N_4, SiO_xN_y and SiO_2 networks, respectively.
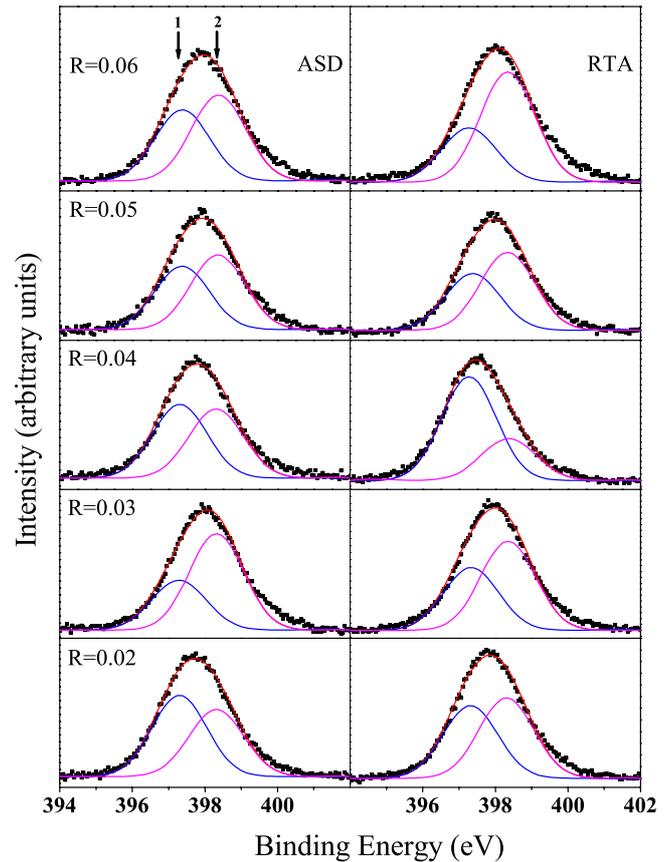

Figure 3. N 1s XPS spectra of ASD and RTA films for different values of gas flow rate ratio R. The experimental data has been deconvoluted into peaks 1 and 2 corresponding to N in Si_3N_4 and SiO_xN_y networks, respectively.

As seen in figure 2, the deconvolution consists of five components: the first two peaks 1 and 2 centered at 99.4 and 100 eV were attributed to elemental Si and are a spin–orbit doublet, $2p_{1/2}$, $2p_{3/2}$, whose splitting is 0.6 eV. The other three peaks 3, 4 and 5 centered around at 101.6 eV, 102.6 eV and 103.6 eV are attributed to Si coordinated in Si_3N_4, SiO_xN_y and SiO_2 networks, respectively. The binding energy position of each peak is in good agreement with the reported values [24–27]. From figure 2, it is clear that all ASD and RTA films have peaks corresponding to Si–Si coordination, Si_3N_4, SiO_xN_y and SiO_2 phases, respectively, having different peak areas. Similarly, as shown in figure 3, the N 1s peak was deconvoluted into two peaks 1 and 2 centered at 397.3 eV and 398.3 eV, which are attributed to coordination of N in Si_3N_4 and SiO_xN_y networks, respectively.

The presence of SiO_xN_y and SiO_2 peaks in Si 2p XPS spectra (figure 2) and the SiO_xN_y peak in N 1s XPS spectra (figure 3) clearly reveals that, at least on the surface, there is significant incorporation of oxygen in all films. The appearance of oxygen, in general, is because of surface oxidation, the presence of residual oxygen/water vapor in the chamber, which can be incorporated during deposition or annealing. Therefore our XPS analysis suggests that, in ASD films, some of the nitrogen in the silicon nitride (a-SiN_x:H) is

substituted by oxygen, resulting in sub-oxide (SiO_x) and sub-oxynitride (SiO_xN_y) type phases. Vila *et al* have also reported the presence of silicon dioxide (SiO_2) and silicon oxynitride (SiO_xN_y) phases in silicon nitride films [27]. Individual phases, namely Si–Si coordination, Si_3N_4, SiO_xN_y and SiO_2 (quantified as integrated intensity of individual deconvoluted peaks from figure 2), are plotted against the reactant gas flow rate ratio for both ASD and RTA films in figure 4. In both ASD and RTA films, the excess silicon/Si–Si coordination content is maximum for $R = 0.04$ (figure 4(a)). In addition, after thermal treatment, except for $R = 0.04$, in all films the contributions of the SiO_2 phase increases whereas that of SiO_xN_y shows a moderate enhancement or remains the same (figures 4(c) and (d)). The contribution of the Si_3N_4 phase either decreases or remains the same upon RTA treatment.

Now we address the question of phase separation in the films under study. In principle as gas flow rate ratio (R) increases the content of Si should also increase; however, the aforementioned XPS results show phase formation/separation of different silicon phases. For the $R = 0.04$ film XPS results show almost double the Si content than the rest of the films. Here it should be pointed out that films corresponding to $R = 0.05$ and 0.06 should have more Si compared to $R = 0.04$ and any excess Si could be detected even in amorphous form by techniques like XPS. Also the refractive indices corresponding
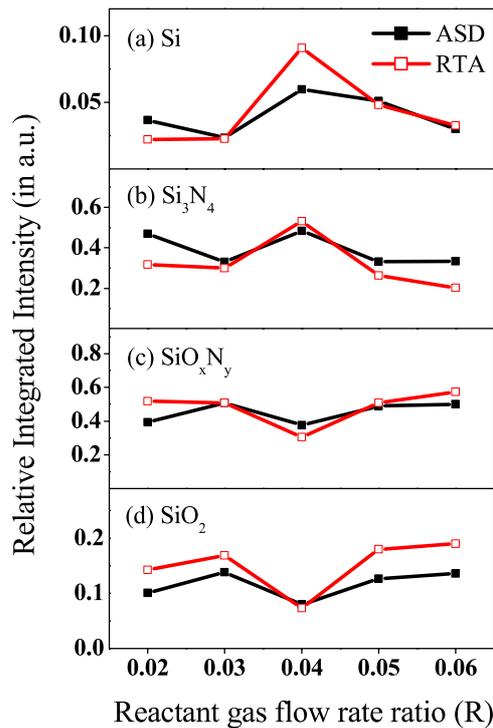
Figure 4. Integrated intensity of Si 2p peak as a function of gas flow rate ratio R for (a) elemental Si, (b) Si_3N_4, (c) SiO_xN_y, (d) SiO_2 networks, respectively.

to $R = 0.05$ and 0.06 after annealing are not very different from those observed for $R = 0.04$. Taking into account all measurements, it can be speculated that the initial amount of hydrogen in the film is playing some role as far as phase separation is concerned. The ASD film corresponding to $R = 0.04$ has minimum concentration of hydrogen in it, though on RTA treatment all films have more or less the same hydrogen concentration. It is already reported that close to stoichiometric silicon nitride films have less concentration of hydrogen [28]. In the present case, from the XPS measurements it was found that the film corresponding to $R = 0.04$ has a dominant silicon nitride phase before and after RTA. Therefore, as compared to other films, $R = 0.04$ films, the least number of bonds involving H (Si–H, N–H) would be broken on RTA, making formation of SiO_2 or SiO_xN_y phases less probable. This is in accordance with the results obtained from XPS data analysis. The less incorporation of hydrogen in the as-deposited films not only helps in the stabilization of the silicon nitride phase but also enable unreacted Si atoms to cluster before and after RTA, resulting in the observed phase separation. Very recently, Daldosso *et al* and Molinari *et al* have also pointed out that hydrogen and nitrogen atoms play a key role in the formation of Si clusters and structural evolution of the host matrix [7, 29]. As mentioned in their work we also believe that the proposed process could occur at relatively low Si concentrations, as is the present case, but if one keeps on increasing the volume fraction of Si, ultimately Si will recrystallize into c-Si in a silicon nitride matrix. Therefore, it is clear that the initial hydrogen concentration in as-deposited samples, rather than simply the reactant gas flow ratio (R), plays a vital role in

phase stabilization. However, as the current study is based on films with limited variation in R (0.02–0.06), a wide range of datasets is required for further confirmation and such studies are under progress.

4. Conclusions

Systematic experiments were performed on various hydrogenated amorphous silicon nitride (a-SiN_x:H) films formed by photo-CVD to examine the changes in structural and optical features upon thermal treatment. RTA-treated films showed substantial densification (up to 29% reduction) and large changes in refractive index (up to 22% enhancement). It is clear that a mere change in the initial deposition parameters would not simply result in silicon-rich a-SiN_x:H films. Our results are a clear indicative that out-diffusion of hydrogen takes place upon RTA treatment. Also, the surface of a-SiN_x:H films is composed of various structural phases, namely Si–Si coordination, Si_3N_4, SiO_xN_y and SiO_2. Moreover, their relative contribution is largely different after annealing. It is proposed that hydrogen plays a key role in the overall structural evolution of the host matrix. It is speculated that less incorporation of hydrogen in as-deposited films not only helps in the stabilization of the silicon nitride phase but may also enable unreacted Si atoms to cluster before and after RTA, resulting in the observed phase separation. These studies are of great help and are vital in silicon photonics where the post-treatment of silicon-rich devices is essential.

References

[1] Pavesi L, Dal Negro L, Mazzoleni C, Franzò G and Priolo F 2000 *Nature* **408** 440–4
[2] Cullis A G and Canham L T 1991 *Nature* **353** 335–8
[3] Walters R J, Kalkman J, Polman A, Atwater H A and de Dood M J A 2006 *Phys. Rev.* B **73** 132302
[4] Iacona F, Fanzò G and Spinella C 2000 *J. Appl. Phys.* **87** 1295
   Vinciguerra V, Franzò G, Priolo F, Iacona F and Spinella C 2000 *J. Appl. Phys.* **87** 8165–73
[5] Chen L Y, Chen W H and Hong F C 2005 *Appl. Phys. Lett.* **86** 193506
[6] Torchynskaa T, Becerril Espinoza F G, Goldstein Y, Savir E, Jedrzejewski J, Khomenkova L, Korsunska N and Yukhimchukc V 2003 *Physica* B **340** 1119–23
[7] Daldosso N, Das G, Larcheri S, Mariotto G, Dalba G, Pavesi L, Irrera A, Priolo F, Iacona F and Rocca F 2007 *J. Appl. Phys.* **101** 113510
[8] Min K S, Shcheglov K V, Yang C M, Atwater Harry A, Brongersma M L and Polman A 1996 *Appl. Phys. Lett.* **69** 2033–5

 [9] Wang Y, Shen D, Liu Y, Zhang J, Zhang Z, Liu Y, Lu Y and
      Fan X 2005 *Physica* E **27** 284–9
[10] Ma K, Feng J Y and Zhang Z J 2006 *Nanotechnology*
      17 4650–3
[11] Thakur R P S and Singh R 1994 *Appl. Phys. Lett.* **64** 327–9
[12] Augustine B H, Hu Y Z, Irene E A and McNeil L E 1995
      Appl. Phys. Lett. **67** 3694–6
[13] Mei J J, Chen H, Shen W Z and Dekkers H F W 2006 *J. Appl.
      Phys.* **100** 073516
[14] Maedaa M and Itsumi M 1998 *J. Appl. Phys.* **84** 5243–7
[15] Beshkov G, Dimitrov D B, Velchev N, Petrov P, Ivanov B,
      Zambov L and Dimitrova T 2000 *Vacuum* **58** 509–15
[16] Singh S P, Srivastava P, Prakash G V, Modi M H, Rai S and
      Lodha G S 2008 *J. Phys.: Condens. Matter* **20** 335232
[17] Rathi K, Gupta M, Thangaraj R, Chari K S and Agnihotri O P
      1995 *Thin Solid Films* **266** 219–23
[18] Ghosh S, Ingale A, Som T, Kabiraj D, Tripathi A, Mishra S,
      Zhang S, Hong X and Avasthi D K 2001 *Solid State
      Commun.* **120** 445–50
[19] Sahu B S, Srivastava P, Agnihotri O P, Lee H C, Sekhar B R,
      Mahapatra S and Tiwari M K 2004 *Thin Solid Films*
      446 23–8
[20] Mittal V K, Lotha S and Avasthi D K 1999 *Radiat. Eff. Defects
      Solids* **147** 199
[21] Akazawa H 2002 *Appl. Phys. Lett.* **80** 3102–4
[22] Modi M H, Lodha G S, Srivastava P, Sinha A K and
      Nandedkar R V 2006 *Phys. Rev.* B **74** 045326
[23] Cai L, Rohatgi A, Yang D and El-Sayed M A 1996 *J. Appl.
      Phys.* **80** 5384–8
[24] Li B, Fujimoto T, Fukumoto N, Honda K and Kojima I 1998
      Thin Solid Films **334** 140–4
[25] Tsu D V, Lucovsky G, Mantini J and Chao S S 1987 *J. Vac. Sci.
      Technol.* A **5** 1998–2002
[26] Taylor T N, Butt D P and Pantano C G 1998 *Surf. Interface
      Anal.* **26** 134–43
[27] Vila M, Román E and Prieto C 2005 *J. Appl. Phys.* **97** 113710
[28] Rathi V K 1994 Photodeposition of silicon nitride and study of
      its interface properties *Thesis*
[29] Molinari M, Rinnert H and Vergnat M 2007 *J. Appl. Phys.*
      101 123532